PERGAMON

International Journal of Heat and Mass Transfer 44 (2001) 1649–1657

International Journal of HEAT and MASS TRANSFER

www.elsevier.com/locate/ijhmt

Photophoresis of micrometer-sized particles in the free-molecular regime

Shahram Tehranian [a], Frank Giovane [b], Jürgen Blum [b,c,*], Yu-Lin Xu [c], Bo Å.S. Gustafson [c]

[a] *Institute for Computational Sciences and Informatics, MS5C3, George Mason University, Fairfax, VA 22030-4444, USA*
[b] *Space Science Division, Naval Research Laboratory, 4555 Overlook Avenue SW, Washington, DC 20375-5320, USA*
[c] *Department of Astronomy, P.O. Box 112055, University of Florida, Gainesville, FL 32611-2055, USA*

Received 12 April 2000; received in revised form 30 June 2000

Abstract

The photophoretic force in the free-molecular regime has been calculated for a spherical particle using the Lorenz–Mie solution to the electromagnetic field within the particle. The temperature distribution on the surface of the suspended particle is calculated using a finite difference method. The effect of the complex refractive index $m = n + ik$ and the normalized size parameter defined as $\alpha = 2\pi a/\lambda$ on the photophoretic force and particle velocity are also examined. We show that for a 1 solar constant illumination, the photophoretic forces might be as high as 20% of the weight of the particles considered. © 2001 Published by Elsevier Science Ltd.

1. Introduction

Photophoresis owes its existence to a non-uniform temperature distribution of an illuminated particle in a gaseous medium. Although the photophoretic effect has been known for long time, there is a multitude of recent publications on the general phenomenon [1], introducing complex particle structures [2,3] or transient heating [4]. Photophoresis has important applications in particle trapping and levitation [5,6], in the field-flow fractionation of particles [7], in the determination of the thermal conductivity and temperature of microscopic grains [8,9], and in the transport of soot particles in the atmosphere [10,11].

In a discussion of radiometric forces, it is convenient to recognize three different flow regimes depending on the pressure of the gas and the size of the suspended particle. The similarity parameter that governs these different regimes is the Knudsen number, defined as $Kn = l/a$, where l is the average mean free path of the gas molecules and a is the radius of the sphere. The photophoretic force increases as the presssure is reduced in the continuum regime where the Knudsen number $Kn \ll 1$. It reaches its maximum value in the transition regime when $Kn \sim 1$. As the pressure is further decreased, the photophoretic force will decrease proportionally with the gas pressure. This regime is called the free-molecular regime where the Knudsen number Kn is much greater than one. For the situation where the average mean free path of the gas molecules is much larger than the particle radius, that is for high Knudsen number flows, the photophoretic force can be calculated by considering the momentum transfer to and from the surface of the particle [12–14]. For gas-suspended spherical particles, photophoresis may result in a particle movement either away from or toward the light source. For positive photophoresis, the illuminated side is hotter and the movment is in the direction of the light beam; for negative photophoresis, the shaded side is hotter and the particle moves toward the light source.

2. Theory

The uneven temperature distribution on the surface of the particle depends on the source function

* Corresponding author.

0017-9310/01/$ - see front matter © 2001 Published by Elsevier Science Ltd.
PII: S0017-9310(00)00230-1

Nomenclature

A	sphere radius
B	non-dimensional electric field distribution function
c_p	specific heat of the particle
D	aerodynamic drag
E	electric field distribution function
E_0	incident electric field strength
F_p	photophoretic force
H	energy flux
I	light source intensity
k	imaginary part of the complex refractive index
k_p	thermal conductivity of the particle
Kn	Knudsen number
l	average mean free path of the gas molecules
m	complex refractive index
n	real part of the complex refractive index
P	gas pressure
Q	heat generation function
r	radial direction
R	specific gas constant
T	temperature
$\bar{u}$	average molecular speed of gas molecules
V_p	photophoretic velocity
X, Y, Z	rectangular coordinates

Greek symbols

α	normalized size parameter
ϵ	emissivity of the particle
θ	elevation angle
λ	wavelength of the light source
μ	dynamic viscosity of the gas
ρ	density
σ	Stefan–Boltzmann constant
ϕ	azimuthal angle

Subscripts

c	conduction
g	gas
i	incident
p	particle
r	reflected
rad	radiation

representing the distribution radiant-energy absorption [15]. This source function is defined as

$$Q(r,\theta) = \frac{4\pi nkI}{\lambda}\frac{|E(r,\theta)|^2}{|E_0|^2} = \frac{4\pi nkI}{\lambda}B(r,\theta), \quad (1)$$

where n and k are the real and imaginary parts of the complex refractive index of the particle, λ the wavelength of the light, I the intensity of the light source and $E(r,\theta)$ is the electric field within the particle. E_0 is the incident electric field strength and $B(r,\theta)$ is the non-dimensional electric field distribution function.

The starting point for a theory of photophoresis must be the determination of this source function in terms of the non-dimensional electric field represented by $B(r,\theta)$ in Eq. (1). The particle geometry and coordinates are depicted in Fig. 1. In this figure, a monochromatic, parallel, linearly polarized wave propagating along the Z-axis illuminates the spherical particle.

For micron-sized particles where the radius of the particle is comparable to the wavelength of the light source, the radiation absorption will be distributed within the entire volume of the illuminated particle [16,17]. For a highly absorbing particle with a diameter much larger than the wavelength λ, the absorption of the energy will most likely occur on the illuminated surface and in the irradiated hemisphere with a resulting force directed away from the light source. This is referred to as positive photophoresis. For a less absorbing particle however, the irradiated energy can be deposited anywhere within the particle depending on the normalized size parameter $\alpha = 2\pi a/\lambda$ and the complex refractive index $m = n + ik$ of the particle. This may result in a negative photophoretic force if the shaded particle surface and hemisphere absorb most of the radiation, in which case the particle moves toward the light source.

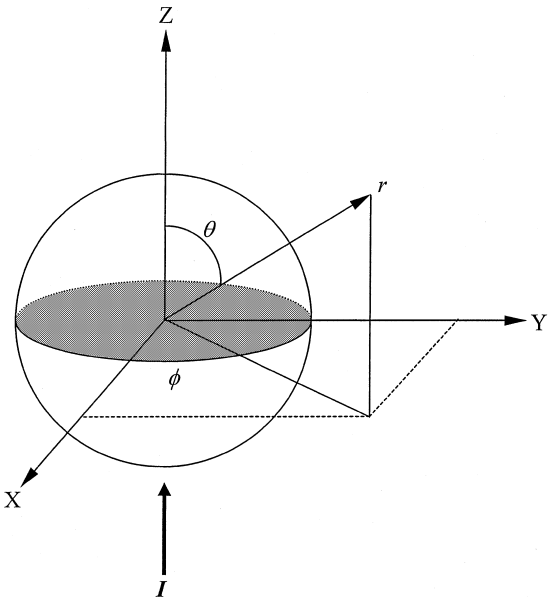

Fig. 1. Geometry of illuminated particle for analysis.

The internal electrical field was calculated through the use of Ricatti–Bessel functions, Legendre functions, and their derivatives. To obtain a sufficiently accurate internal field distribution for spherical particles in practical calculations, reliable numerical techniques are of crucial importance. Minor errors in the total rate of energy absorption will completely distort the temperature distribution within a particle and the associated photophoretic force. The normalized source function $Q(r,\theta)$ given by Eq. (1) depends strongly on the size parameter and the complex refractive index of the illuminated sphere. The pattern of the distribution of absorption centers in the sphere changes dramatically with the change in size and refractive index. Fig. 2 shows the non-dimensional electric field $B(r,\theta)$ for the X–Z plane ($\phi = 0$) of the particle for different size parameters and refractive indices (mind that for a better perspective, the r and θ axes are exchanged in Figs. 2(c) and (d) with respect to Figs. 2(a) and (b)). The electric field vector points in the Y-direction and the light is propagating in the Z-direction from negative (at the front side of the particle) to positive (at the back side of the particle). Since the present work aims at the photophoretic behavior of spherical particles, we only give brief description of the trends of the source function in terms of the non-dimensional electrical field. The calculation of the heat source function both for single spheres and for aggregates has been studied extensively by [3].

The non-dimensional electric field for a size parameter of 2.0 and a refractive index of $m = 1.95 - 0.3\mathrm{i}$ is shown in Fig. 2(a). For this combination of size parameter and refractive index, the electric field is clearly dominant on the shaded side of the particle. This would result in what is termed as negative photophoresis. Recall from Fig. 1 that $\theta = 0$ corresponds to the shaded side of the illuminated particle. In Fig. 2(b), the refractive index of the particle is kept constant while the size parameter α is increased to a value of 2.6. In this case, both the illuminated and the shaded hemisphere of the particle absorb radiation, with the highest absorption

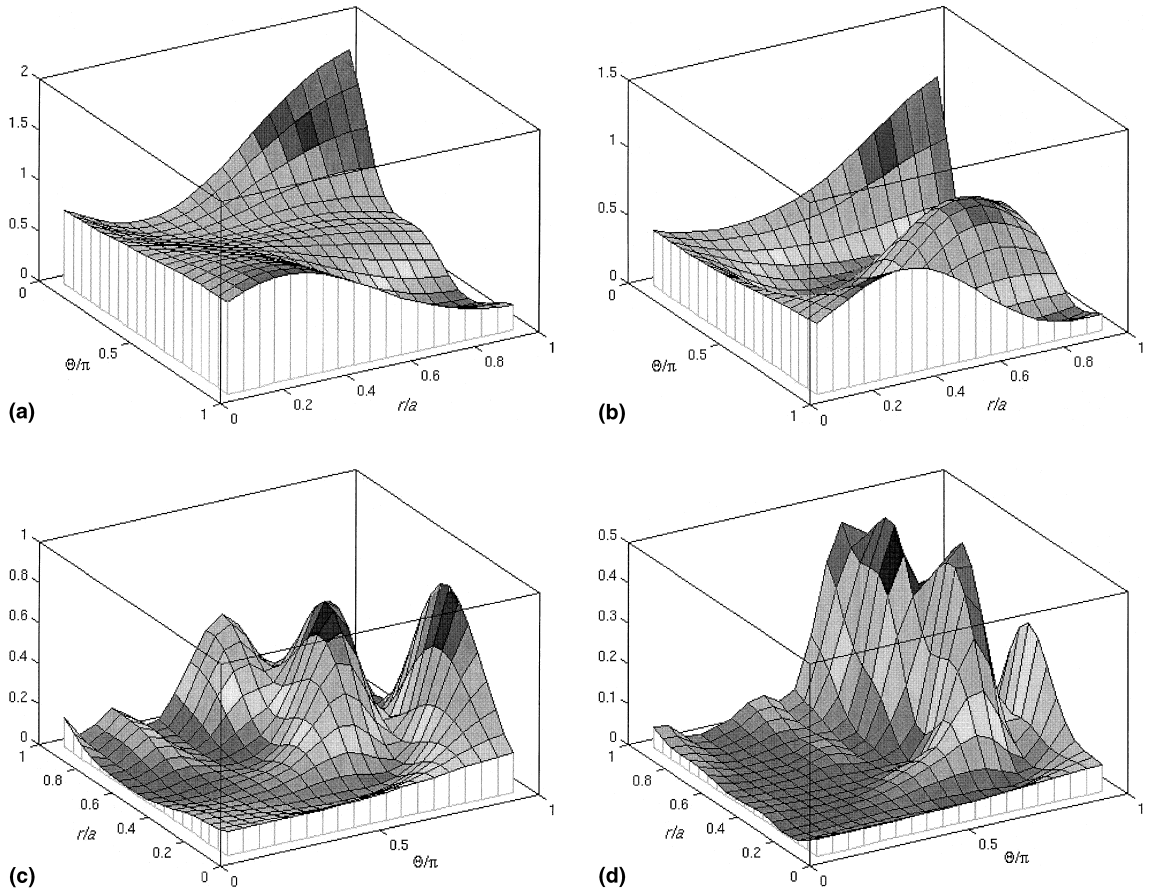

Fig. 2. Non-dimensional electric field $B(r,\theta)$ for a sphere having a size parameter α and a refractive index m of: (a) $\alpha = 2.0$, $m = 1.95 - 0.3\mathrm{i}$; (b) $\alpha = 2.6$, $m = 1.95 - 0.3\mathrm{i}$; (c) $\alpha = 4.0$, $m = 1.95 - 0.3\mathrm{i}$; (d) $\alpha = 6.0$, $m = 1.95 - 0.3\mathrm{i}$. Mind that for a better perspective, the r and θ axes are exchanged in (c) and (d) with respect to (a) and (b).

remaining in the shaded hemisphere. As the size parameter is further increased, the absorption in the illuminated hemisphere is strongly accentuated while the absorption in the non-illuminated hemisphere becomes negligible. This is shown in Figs. 2(c) and (d). Hence the photophoretic force changes its direction from negative to positive.

Although the internal field distribution and thus the direction and magnitude of the photophoretic force are highly dependent on the physical parameters of the particles, changing from particle to particle, some conclusions may nevertheless be drawn. For highly absorptive particles, that is, spheres having a large value of the imaginary part of the refractive index, the incident radiation can hardly penetrate, and absoption occurs principally on the illuminated surface and in the illuminated hemisphere of the particle. For highly absorptive particles of a large-size parameter, the illuminated surface and hemisphere absorb most of the radiation, leading to positive photophoresis. However, it should be noted that the effects of the size parameter, α, the real and imaginary part of the refractive index n and k on the source function are interrelated.

3. Analysis

Consider a spherical particle of radius a suspended in gas with a pressure P_g and a temperature T_g and illuminated by a light beam of intensity I. It is assumed that the direct interaction of the light source with the surrounding medium is negligible. The temperature distribution T_p within the suspended particle is governed by the unsteady heat conduction equation given by

$$\rho_p c_p \frac{\partial T_p}{\partial t} = k_p \nabla^2 T_p + Q, \tag{2}$$

where ρ_p, c_p and k_p are the density, specific heat and thermal conductivity of the particle, respectively. Q is the heat source produced by electromagnetic wave absorption defined by Eq. (1).

Neglecting the ϕ dependence of the temperature distribution of the particle and writing the heat conduction equation in spherical coordinates, Eq. (2) takes the form

$$\rho_p c_p \frac{\partial T_p}{\partial t} = k_p \left[\frac{1}{r^2} \frac{\partial}{\partial r} \left(r^2 \frac{T_p}{\partial r} \right) + \frac{1}{r^2 \sin\theta} \frac{\partial}{\partial \theta} \left(\sin\theta \frac{\partial T_p}{\partial \theta} \right) \right] + Q(r,\theta). \tag{3}$$

By using the Maxwellian distribution function for the incident and reflected gas molecules from the surface of the particle, the local energy fluxes can be calculated. The boundary condition on the surface of the illuminated sphere is the sum of the incident energy flux H_i, the reflected energy flux H_r, the heat flux by conduction within the particle H_c, and the heat flux due to radiation to and from the surface of the particle H_{rad}.

Assuming that the surrounding medium is stationary, kinetic theory [18,19] provides rather simple expressions for the energy fluxes of the incident and reflected gas molecules given by Eqs. (4) and (5). The average molecular speed of the gas molecules $\bar{u}$ is given by Eq. (6) with R being the specific gas constant

$$H_i = \frac{1}{2} P \bar{u}, \tag{4}$$

$$H_r = \frac{1}{2} P \bar{u} \left(\frac{T_p}{T_g} \right)^{1/2}, \tag{5}$$

$$\bar{u} = \sqrt{\frac{8RT_g}{\pi}}. \tag{6}$$

The surface radiation energy flux H_{rad} is given by Stefan–Boltzmann law and takes the form

$$H_{rad} = \epsilon\sigma \left(T_p^4 - T_g^4 \right), \tag{7}$$

where the first part represents the radiation from the surface of the particle to the surrounding medium and the second part the radiation from the gas to the particle. The emissivity of the particle is denoted by ϵ and σ is the Stefan–Boltzmann constant. The heat conducted from the particle surface is

$$H_c = -k_p \left(\frac{\partial T_p}{\partial r} \right)_{r=a}, \tag{8}$$

where k_p is the thermal heat conductivity of the particle. Hence the boundary condition at the surface of the particle is given by

$$H_i - H_r - H_{rad} + H_c = 0. \tag{9}$$

Once the heat generation function Q is determined, the temperature distribution T_p within the particle can be calculated through Eq. (3) with the boundary condition given by Eq. (9).

In the free-molecular regime, the incident momentum based on the free-stream gas temperature is uniform over the entire surface of the particle and it makes zero contribution to the force. It is the uneven reflected momentum that results in the photophoretic force. Assuming that all the molecules are reflected diffusely from the surface of the particle, the pressure due to reflected molecules is given by

$$P_r = \frac{1}{2} P \left(\frac{T_p}{T_g} \right)^{1/2}. \tag{10}$$

Hence the photophoretic force will take the form

$$F_p = -\pi a^2 P \int_0^\pi \left(\frac{T_p}{T_g} \right)^{1/2} \cos\theta \sin\theta \, d\theta, \tag{11}$$

where the sign of the force is chosen such that F_p is considered positive in the direction of the propagating light. The photophoretic velocity V_p can be obtained by equating the photophoretic force given by Eq. (11) to the local aerodynamic drag on the body. The aerodynamic drag on the spherical particle is expressed as

$$D = \frac{6\pi\mu V_p a}{1 + Kn(c_1 + c_2 e^{-c_3/Kn})}, \tag{12}$$

where $c_1 = 1.20,\ c_2 = 0.41$, and $c_3 = 0.88$ [15].

4. Results

The temperature distribution for a spherical particle with a refractive index of $m = 1.95 - 0.3i$ and two different size parameters is shown in Fig. 3 (mind that for a better perspective, the r and θ axes are exchanged in Fig. 3(b) with respect to Fig. 3(a)). The non-dimensional electric field $B(r, \theta)$ for the same combination of size parameter and refractive index was previously shown in Figs. 2(a) and (d). The normalized size parameter α is varied from 2 to 6 while the gas pressure is kept constant at 10 Torr or 1330 Pa. The light intensity is put equal to the solar constant, 1353 W/m^2. The specific heat c_p, particle density ρ_p, thermal conductivity k_p and gas temperature T_g are 840 J/kg K, 1900 kg/m^3, 5.0 W/mK, and 273 K, respectively. For the particle considered, the angle $\theta = 0$ corresponds to the shaded or non-illuminated side of the particle, while $\theta = \pi$ represents the front surface of the sphere. For the first case with a size parameter of 2.0, the absorption center is located on the shaded side of the particle, resulting in higher temperatures on the non-illuminated hemisphere as shown in Fig. 3(a). Hence a negative photophoretic force is exerted. As the normalized size parameter is increased to a value of 6, the absorption peaks will move towards the front side of the suspended particle as shown in Fig. 2(d). This behavior is clearly demonstrated in Fig. 3(b) showing higher temperatures on the front side of the particle. Hence a positive photophoretic force is obtained. Note that the difference between the temperature within the particle and the gas temperature, $T_p - T_g$ ranges only from 0.04 to 0.05 K. Hence a small temperature difference is sufficient to induce a photophoretic force on the spherical particle.

Fig. 4 shows the behavior of the photophoretic force for various refractive indices versus the normalized size parameter α. In Fig. 4(a), the photophoretic force F_p is shown for two different refractive indices versus the size parameter. In this case, the imaginary part of the refractive index k is kept constant at a value of 0.001 while the real part n is increased from a value of 1.33 to 1.95. The photophoretic force is negative almost over the entire range of size parameters considered both for $m = 1.33 - 0.001i$ and $1.95 - 0.001i$. For $m = 1.33 - 0.001i$, the magnitude of the photophoretic force increases smoothly with α up to a size parameter of 5.0, where oscillations start to occur. For $m = 1.95 - 0.001i$, the oscillations start to occur at a value of $\alpha = 2.5$. Hence for higher values of the real part of the refractive index, the onset of oscillations occur at lower values of the size parameter. Furthermore for small values of the size parameter, the higher the real part of the refractive index, the larger is the magnitude of the photophoretic force.

Increasing the imaginary part of the refractive index to a value of 0.05, the oscillatory behavior of the photophoretic force is even more dominated. This is shown in Fig. 4(b) for $m = 1.33 - 0.05i$ and $1.95 - 0.05i$. In Fig. 4(c), the imaginary part of the refractive index is further increased to a value of 0.3. Here the photophoretic force is initially negative for the smallest values of the size parameter and then becomes positive with

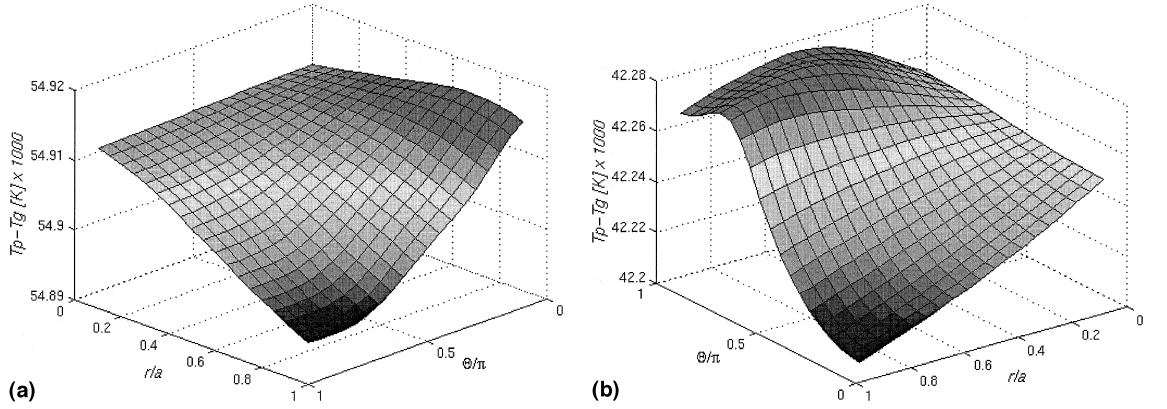

Fig. 3. Temperature distribution inside a spherical particle having a size parameter α and a refractive index m of: (a) $\alpha = 2.0,\ m = 1.95 - 0.3i$; (b) $\alpha = 6.0,\ m = 1.95 - 0.3i$. Mind that for a better perspective, the r and θ axes are exchanged in (b) with respect to (a).

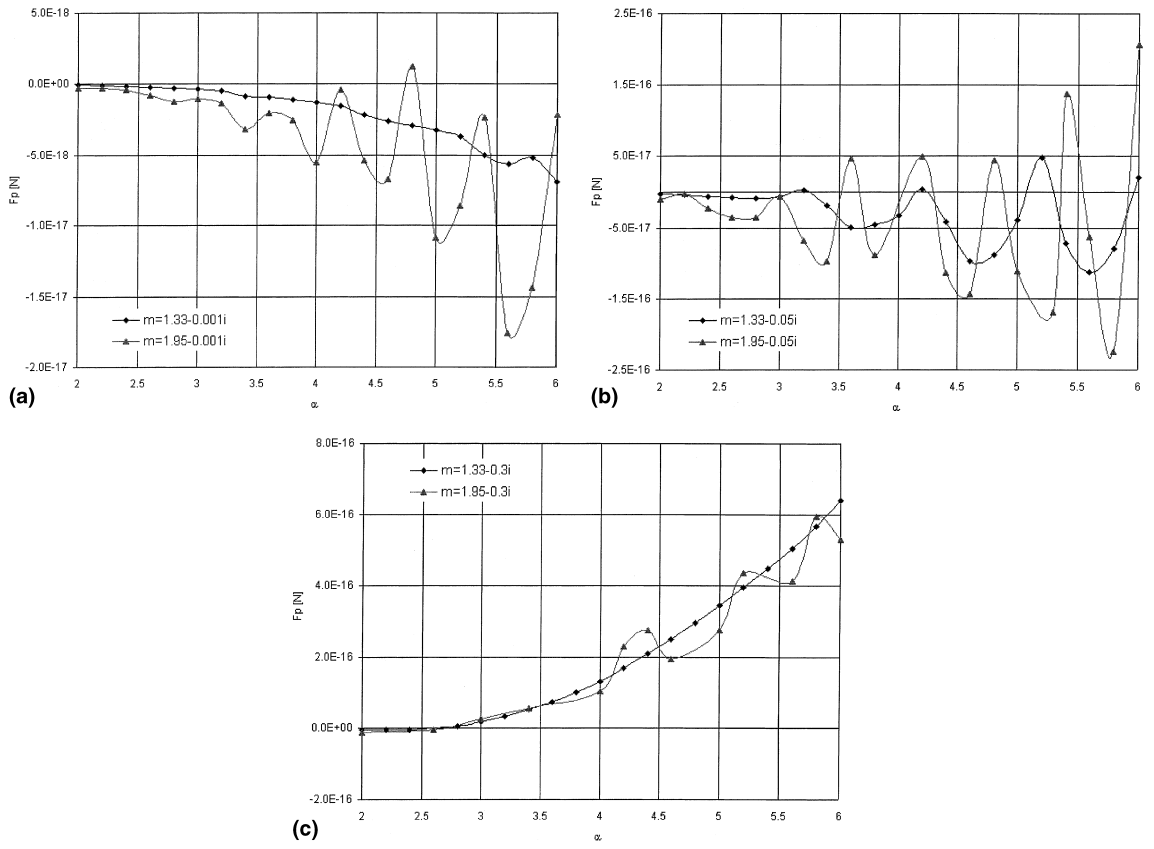

Fig. 4. Photophoretic force F_p versus size parameter α for refractive indices (a) $m = 1.33 - 0.001i,\ 1.95 - 0.001i$; (b) $m = 1.33 - 0.05i,\ 1.95 - 0.05i$; (c) $m = 1.33 - 0.3i,\ 1.95 - 0.3i$.

increasing α. For $m = 1.33 - 0.3i$, the oscillations are completely damped out while there still remains some oscillations for $m = 1.95 - 0.3i$. For these highly absorptive particles with a large size, the incident radiation can hardly penetrate and the absorption occurs only in the front hemisphere of the particle, leading to positive photophoresis. Please note that the magnitude of the photophoretic force has increased with increasing k for these combinations of refractive index and size parameter.

Fig. 5 shows the photophoretic force to weight ratio F_p/W_p versus the normalized size parameter for $m = 1.33 - 0.3i$ and $1.95 - 0.3i$. It is interesting to note that for a refractive index of $1.95 - 0.3i$ and a normalized size parameter of 4.4, the photophoretic force might be as high as about 20% of the weight of the particle considered. It is the authors' belief that even larger forces might be obtained with more suitable combinations of the refractive index and size parameter.

The photophoretic velocity V_p is obtained by equating the photophoretic force given by Eq. (11) to the local aerodynamic drag on the body given by Eq. (12). The sign convention on the photophoretic velocity V_p is chosen such that a particle movement in the direction of the light source is considered positive. Fig. 6 shows the photophoretic particle velocity for various refractive indices versus the size parameter. Since the particle velocity V_p is directly proportional to the photophoretic force through Eq. (12), it exhibits similar behavior as the photophoretic force. The highest photophoretic particle velocity obtained is about 8×10^{-6} m/s for a refractive index of $1.95 - 0.3i$ and a size parameter of 5.8.

In Fig. 7, the present work is compared to the results of Kerker and Cook [19]. In this figure, the photophoretic force is calculated based on the same parameters as given by [19]. The normalized size parameter α is varied from 2 to 6 while the gas pressure is kept constant at 10 Torr or 1330 Pa. The light intensity is put equal to the solar constant, 1353 W/m^2. The light wavelength λ, specific heat c_p, particle density ρ_p, thermal conductivity k_p and gas temperature T_g are 0.6 μm, 840 J/kg K, 1900 kg/m^3, 5.0 W/mK, and 273 K, respectively.

Although the trends and the behavior of the potophoretic force calculated in the present work are quite similar to the results presented by [19], the magnitude of the photophoretic force does not seem to

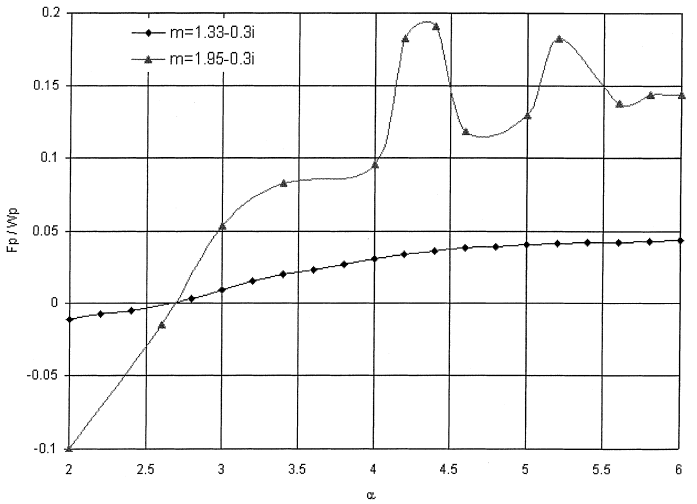

Fig. 5. Photophoretic force to particle weight ratio F_p/W_p versus size parameter α for refractive indices $m = 1.33 - 0.3i,\ 1.95 - 0.3i$.

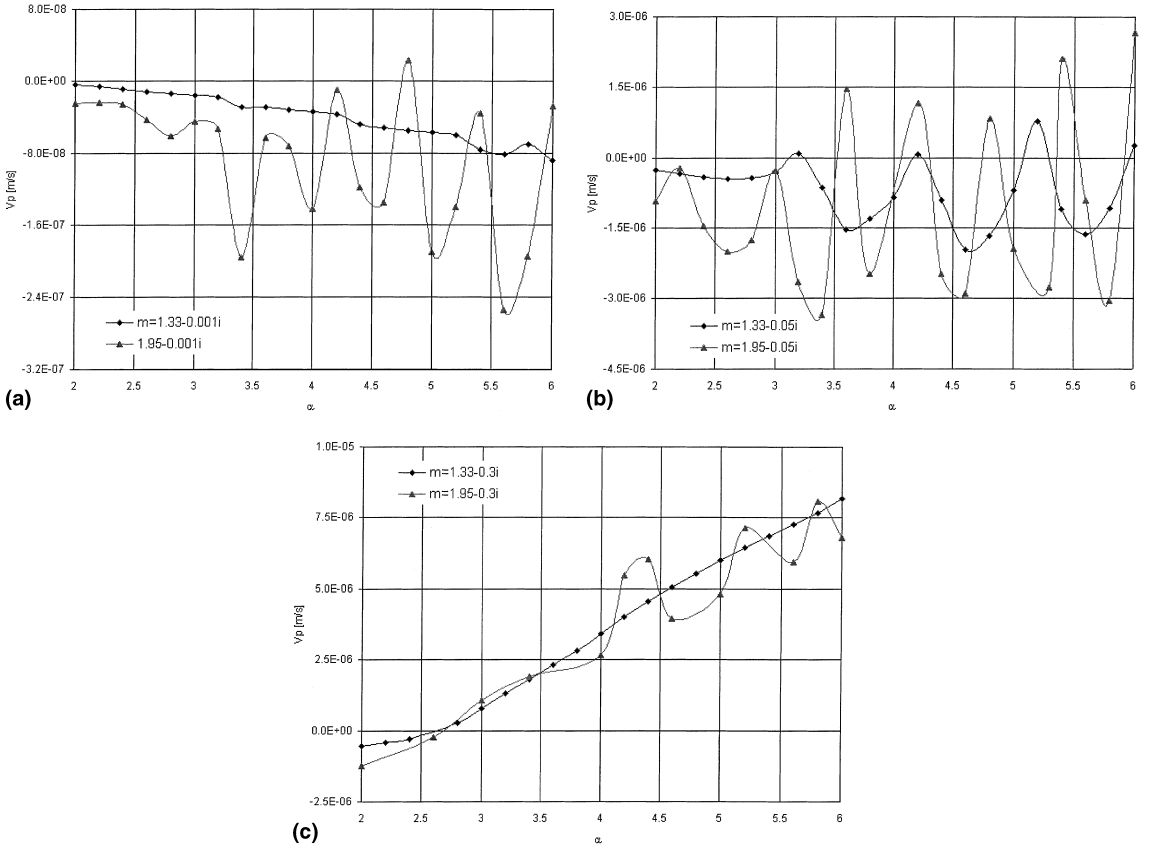

Fig. 6. Photophoretic particle velocity V_p versus size parameter α for refractive indices (a) $m = 1.33 - 0.001i,\ 1.95 - 0.001i$; (b) $m = 1.33 - 0.05i,\ 1.95 - 0.05i$; (c) $m = 1.33 - 0.3i,\ 1.95 - 0.3i$.

match. It is interesting to note that the calculated photophoretic forces by [19] are about 2×10^4 smaller than the results in the present work. Kerker and Cook [19] state that their calculated photophoretic forces are within 2–4% of the gravitational forces in the size range $\alpha = 3$–4 for particles with the densities of carbon and

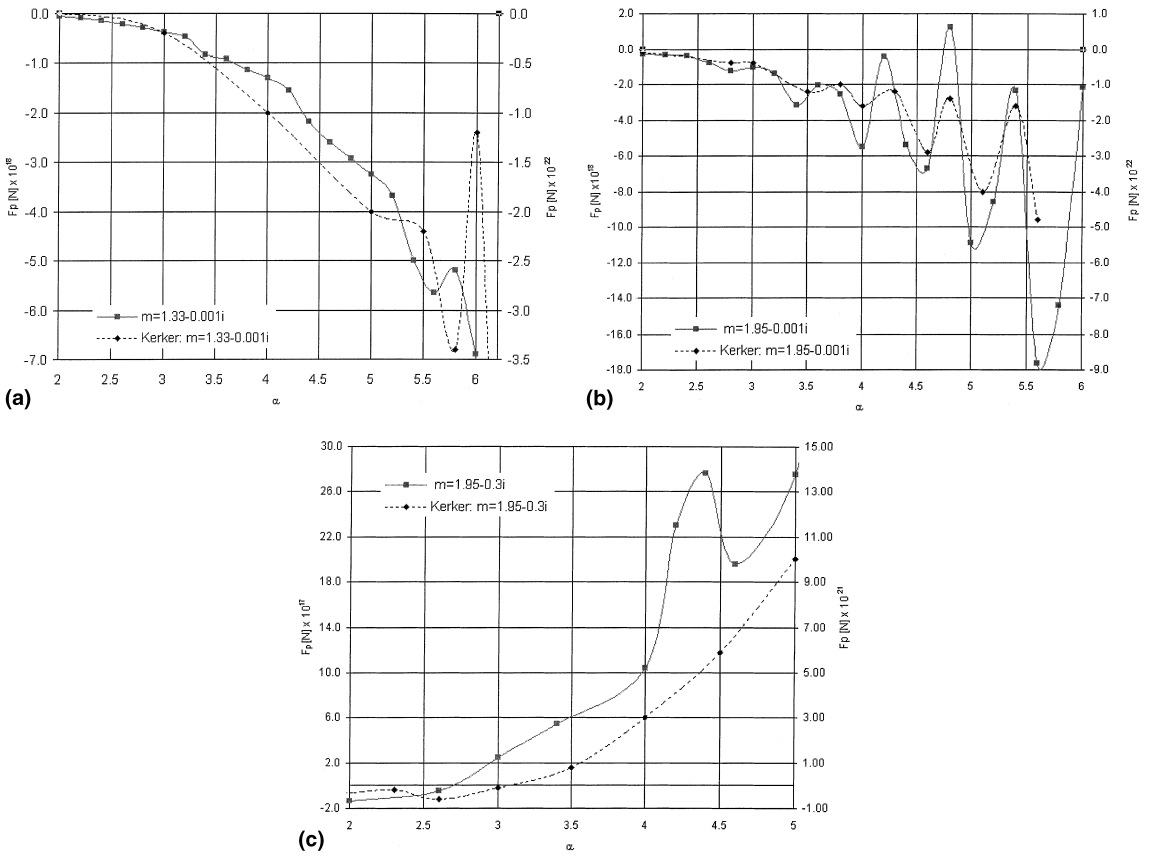

Fig. 7. Comparison of the present work with the results of [19]. Photophoretic force F_p versus size parameter α for a refractive index of $m = 1.33 - 0.001i$; (b) of $m = 1.95 - 0.001i$; (c) of $m = 1.95 - 0.3i$.

water. For a particle density of 1900 kg/m^3, a light wavelength of 0.6 μm, and a size parameter of 4, the particle weight is 4.4×10^{-15} kg. Assuming that the photophoretic forces are 2–4% of the weight of the particle, F_p ranges from 8.7×10^{-17} to 1.7×10^{-16} and is not the order of 10^{-21}–10^{-22} as presented by Kerker and Cook [19]. Hence it is believed that Kerker and Cook [19] made an error in presenting their results. Disregarding the differences in the magnitude of the photophoretic forces, there is good agreement between the present analysis and the work by [19]. However, as the size parameter becomes larger, there appear obvious differences between our results and those of Kerker and Cook [19]. Such an example is shown in Fig. 7(c) where higher oscillations are achieved in our calculations. For a large-size parameter, the calculation of the source function requires the evaluation of higher orders and degrees Ricatti–Bessel functions, which may cause larger numerical errors. This may be the reason that some approximations work reasonably well at low-order function calculations and are not sufficiently accurate at higher orders [3].

5. Conclusions

In this study, we have calculated the photophoretic forces on spherical particles of various refractive indices and size parameters in the free-molecular flow regime and for 1 solar constant illumination. It has been shown that for specific refractive indices and size parameters, the photophoretic force can amount to as much as 20% of the particle weights; this means that a substantial size/refractive index discrimination may occur in natural or artificial environments such as the upper atmosphere or in experiments under reduced gravity conditions.

Although absolute particle velocities due to photophoresis are quite small (few microns/s), the net effect of an additional particle motion may not be negligible; for micron-sized particles, the velocity due to Brownian motion is typically 1 mm/s and thus much larger than the photophoretic velocity; however, photophoresis is a directed motion whereas thermal motion is a diffusive motion, so that the drift distance due to photophoresis might be substantially larger than the thermal diffusion.

Acknowledgements

This work was supported by NASA grant N00173-99-1-G019.

References

[1] S. Beresnev, V. Chernyak, G. Fomyagin, Photophoresis of a spherical-particle in a rarefield gas, Phys. Fluids 5 (1993) 2043–2052.
[2] Y.I. Yalamov, A.S. Khasanov, Photophoresis of coarse aerosol particles with nonuniform thermal conductivity, Tech. Phys. 43 (1993) 347–352.
[3] Y.-L. Xu, B.A.S. Gustafson, F. Giovane, J. Blum, S. Tehranian, Calculation of the heat-source function in photophoresis of aggregated spheres, Phys. Rev. E 60 (1999) 2347–2365.
[4] W.R. Foss, F.J. Davis, Transient laser heating of single solid microspheres, Chem. Eng. Commun. 153 (1996) 113–138.
[5] A. Hirai, H. Monjushiro, H. Watarai, Laser photophoresis of a single droplet in oil in water emulsions, Langmuir 12 (1996) 5570–5575.
[6] M. Rosenberg, D.A. Mendis, D.P. Sheehan, Positively charged dust crystals induced by radiative heating, IEEE Trans. Plasma Sci. 27 (1999) 239–242.
[7] V.L. Kononenko, J.K. Shimkus, J.C. Giddings, M.N. Myers, Feasibility studies on photophoretic effects in field-flow fractionation of particles, J. Liquid Chromatogr. Related Technol. 20 (1997) 2907–2929.
[8] X.F. Zhang, E. Bar-Ziv, A novel approach to determine thermal conductivity of micron-sized fuel particles, Combust. Sci. Technol. 130 (1997) 79–95.
[9] B. Zhao, D. Katoshevski, E. Bar-Ziv, Temperature determination of single micrometre-sized particles from forced/free convection and photophoresis, Meas. Sci. Technol. 10 (1999) 1222–1232.
[10] H. Rohatschek, Levitation of stratospheric and mesospheric aerosols by gravito-photophoresis, J. Aerosol Sci. 27 (1996) 467–475.
[11] R.F. Pueschel, S. Verma, H. Rohatschek, G.V. Ferry, N. Boiadjieva, S.D. Howard, A.W. Strawa, Vertical transport of anthropogenic soot aerosol into the middle atmosphere, J. Geophys. Res.–Atmos. 105 (D3) (2000) 3727–3736.
[12] N.T. Tong, Photophoretic force in the free molecular and transition regime, J. Colloid Interface Sci. 43 (1973) 78–84.
[13] S.P. Lin, On photophoresis, J. Colloid Interface Sci. 51 (1975) 66–71.
[14] A. Akhtaruzzaman, S.P. Lin, Photophoresis of absorbing particles, J. Colloid Interface Sci. 61 (1977) 170–182.
[15] D.W. Mackowski, Photophoresis of aerosol particles in the free molecular and slip-flow regimes, Int. J. Heat Mass Transfer 32 (1989) 843–854.
[16] W.M. Greene, R.E. Spjut, E. Bar-Ziv, A.F. Sarofim, J.P. Longwell, Photophoresis of irradiated spheres: absorption centers, J. Opt. Soc. Am. B 2 (1985) 998–1004.
[17] P.W. Dusel, M. Kerker, D.D. Cooke, Distribution of absorption centers within irradiated spheres, J. Opt. Soc. Am. 69 (1979) 55–59.
[18] G.A. Bird, Molecular Gas Dynamics and the Direct Simulation of Gas Flows, Oxford University Press, New York, 1995.
[19] M. Kerker, D.D. Cooke, Photophoretic force on aerosol particles in the free molecular regime, J. Opt. Soc. Am. 72 (1982) 843–853.